Journal of Sol-Gel Science and Technology (2021) 97:414–421
https://doi.org/10.1007/s10971-020-05444-3

ORIGINAL PAPER: SOL-GEL AND HYBRID MATERIALS FOR ENERGY, ENVIRONMENT AND BUILDING APPLICATIONS

Investigation of thermal insulation performance of glass/carbon fiber-reinforced silica aerogel composites

Wei-Cheng Hung[1] · Richard S. Horng[2] · Rung-En Shia[2]

Received: 20 August 2020 / Accepted: 10 November 2020 / Published online: 6 December 2020
© Springer Science+Business Media, LLC, part of Springer Nature 2020

Abstract

Silica aerogels have been widely used as thermal insulators, but their fragility has hindered the potential applications. In this work, a novel way of improving aerogel skeletal structure was proposed where composites were reinforced by three functional layers of glass fiber (GF)/ carbon fiber (CF). Heat insulation performance of fiber-reinforced aerogel composites was also investigated in a simulated solar radiation system. Composites composed of three layers of fiber were prepared by a sol-gel process under ambient pressure drying. The results showed that, as three layers were all GF blankets, the composite heat conductivity increased with increasing glass fiber content. Flexural strength increased initially and reached a maximum at 20% glass fiber content before decreasing. To find a balance between promoting heat insulation performance and strengthening the composite structure, two layers of 5% glass fiber blankets were used as structure strengthening layers and one carding 5% carbon fiber as the heat insulation layer were recommended. Under these conditions, the composite showed extremely low thermal conductivity (0.031 W/m K), almost comparable to that of pure aerogel (0.036 W/m K) while maintaining high flexural strength (2.846 MPa), superior than previous studies. Composites with other ratios of glass/carbon fibers with sandwiched alignments also demonstrated better flexural strength and lower thermal conductivity than GF aerogel composites. This work provided an alternative way to prepare robust and sustainable heat insulation aerogel composites for practical uses.

Graphical Abstract

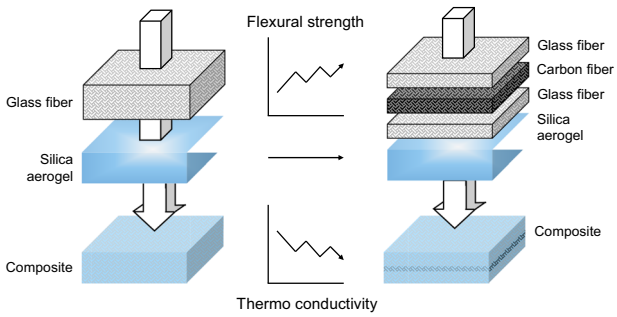

Keywords Silica aerogel · Thermal conductivity · Glass fiber · Carbon fiber · Aerogel composites

✉ Richard S. Horng
richard@isu.edu.tw

[1] Department of Civil and Environmental Engineering, University of California, Los Angeles, Los Angeles, CA 90095, USA

[2] Department of Chemical Engineering, I-Shou University, Kaohsiung City, Taiwan

Highlights

- Heat insulation performance of silica aerogels composited with different ratios of glass fiber and carbon fiber was investigated.
- The flexural strength increased with increased glass fiber loading, and reached its highest value when glass fiber content was 20%.
- 5% carbon fiber inserted between the two 5% glass fiber layers was found the most ideal condition in terms of flexural strength (2.846 MPa) and thermal conductivity (0.031 W/m K).

1 Introduction

With the continual rise of the global energy crisis and greenhouse gas effects, developing highly energy efficient products is necessary. Silica aerogels have been recognized as one of the best high-performance thermal insulation materials. More specifically, silica aerogels, commonly used as potential additives, are widely applied as thermal insulators and fire-resistant materials in buildings. For example, resins replenished with silica aerogels were shown to improve insulation. When resin was applied to an innovative glazing system, where the gap was filled with the resin mixture between glazings, the resulting thermal transmittance (U-value) significantly decreased to 1.05 W/m^2 K due to resin addition [1, 2].

A sol-gel process (gelation, aging, and drying) has been conventionally used to obtain high surface area, high porosity, low density, and high-performance of thermal insulation aerogels. The initial step is to produce a gel through a two-step acid/base catalyzed hydrolysis and condensation of alkoxide precursors, such as tetraethyloorthosilane (TEOS), followed by aging, washing, and drying by either supercritical drying (SCD) or ambient pressure drying (APD) [3–5]. However, due to the fragile nature of aerogels, their nanostructure is often compromised during chemical processing, which may hinder their practical applications. Studies have shown that highly robust aerogel products can be achieved through compounding with polymers or introducing dispersed fibers or fiber mats in the silica aerogel matrix.

Fibers may be composited with aerogels to form fiber-aerogel products for strengthening purposes while maintaining low thermal conductivity. Various fibers have been proposed as reinforcement, including glass fibers (GFs), carbon fibers (CFs), and ceramic fibers [6–8]. For example, GFs-reinforced aerogel blankets have been produced by Aspen Aerogel Inc. and Cabot Corp. Thermal conductivities of composite products with GFs showed low thermal conductivity, ranging from ~0.020 to 0.040 W/m K and 0.020–0.025 W/m K, respectively [9, 10].

To obtain aerogel composites, one common way is to pour the prepared alcosol solution from the silicon precursor into a mold with good fiber dispersion before gelation. The resulting fiber/silica gel was aged, washed, and then dried. Ceramic fibers-reinforced silica aerogels have been previously developed and assessed by [6, 11, 12]. Silica aerogels containing 10% ceramic fibers in volume were proven to significantly improve the compressive strength, from 1.8×10^4 Pa to 12.8×10^4 Pa, and the density, from 0.112 g/cm^3 to 0.185 g/cm^3, with respect to pure aerogel and the reinforced aerogel. Meanwhile, CF is costly but strong, durable, lightweight, and low thermal conductivity. Wei et al [7]. used CFs with amounts from 0.5 to 20% of total weight as reinforcements for silica aerogels. For example, with 20% (w/w) CF addition, as compared to pure aerogel, the composite density, specific surface area, and thermal conductivity dropped from 0.218 to 0.110 g/cm^3, from 1199 to 696 m^2/g, and from 0.041 to 0.0380 W/(m K), respectively. The addition of CFs significantly reduces the density and the specific surface area of the aerogel nanocomposite while thermal conductivity was improved.

In parallel, GF has comparable mechanical properties to CF while being less costly as a reinforcing agent to form composites. Zhou et al [13]. prepared GF-reinforced silica aerogel composites by using methyltrimethoxysilane (MTMS) and water glass co-precursors under freeze drying. The composites displayed remarkable mechanical strength and flexibility, given that the molar ratio of MTMS/water glass (1.8) significantly contributed to composite properties. The elastic modulus and thermal conductivity of the composites were 634.2 kPa and 0.0248 W/m K, respectively. Notwithstanding, these properties are 3184.4 kPa and 0.0295 W/m K when the molar ratio of MTMS/water glass approaches zero. Shafi et al [14]. used fumed silica to improve the insulating and mechanical performance of aerogel/GF composites. The resultant composite possessed extremely low thermal conductivity (0.0194 W/m K), flexural strength (0.58 MPa), and low bulk density (0.239 g/cm^3). Wu et al [8]. developed multilayer GF-reinforced composites by impregnating aligned fibers into aerogels by using sol-gel technique with APD. The thermal conductivity of four-layer aligned fibers with six laminated structures was 0.0233–0.0274 W/m K where pure as-prepared aerogel was 0.0221 W/m K. Meanwhile, the bending strengths were greatly improved from 0.07 to 0.17–0.27 MPa.

Both glass and CFs are commonly used as reinforcements due to their combination of high strength and relatively low density. Besides, fibers can be manipulated in

different forms to reinforce aerogel structures. For instance, blanket forms are known for stronger composite structures as opposed to strand forms. In this work, we aim to prepare reinforced aerogel composites with combined glass/CFs, and with layers of fibers in different forms and functions, while maintaining low thermal conductivity. This study will be beneficial for future industries in preparation of versatile fiber-reinforced aerogels with great insulation characteristics and composite strength.

2 Material and methods

2.1 Raw materials

In this study, GFs (42031/M300, 3421B/M200-GA600, Ahlstrom-Munksjo) and CFs (T300-3000-40A, TORAY TORAYCA) were used as reinforcements. Ethanol (EtOH), n-hexane, hydrochloric acid ($HCl_{(aq)}$, 37% v/v), aqueous ammonia solution ($NH_4OH_{(aq)}$, 27% v/v), TEOS, and trimethylchlorosilane (TMCS) were of chemically-pure grade and purchased from Sigma-Aldrich (St. Louis, MO, USA). Deionized water was utilized to prepare 1 M $HCl_{(aq)}$ and 0.2 M $NH_4OH_{(aq)}$ as the acid and base catalysts.

2.2 Preparation of fiber-aerogel composites

TEOS, EtOH, and H_2O were mixed with water in a molar ratio 1:3:4 in a beaker. The acid catalyst (1 M $HCl_{(aq)}$) was added to the precursor solution. After sufficient hydrolysis (30 min), $NH_4OH_{(aq)}$ (0.2 M) was added into the mixed solution. The obtained silica sol was poured into a rectangular mold with a size of 60 mm × 60 mm × 5 mm (length × width × thickness) for heat conduction measurements and 90 mm × 15 mm × 5 mm (length × width × thickness) for flexural strength measurements, with the fiber layers properly well-dispersed along the length of the mold, and kept for gelation. The generated fiber/alcogels were aged with EtOH for 12 h at 50 °C, exchanged with n-hexane for 12 h and surface modification with TMCS/n-hexane solution at 1:4 volume ratio for 24 h, and washed with ethanol/hexane and then exchanged with hexane. Lastly, the wet alcogel with fiber was dried under ambient pressure and temperature for 3 h, 50 °C for 12 h, and then at 100 °C for an hour. The composites obtained from various fiber contents (by weight shown in Table 1) were then ready for further analyses.

2.3 Characterization of fiber-reinforced aerogel composite

The composite density was measured by the water immersion method according to the American Society for Testing and Materials (ASTM) C-20 method [15]. The surface area of the samples was determined by Brunauer–Emmitt–Teller (BET) analysis with nitrogen adsorption over a range of relative pressures ($0.01 < p/p_0 < 1$) (precision: 0.01 m^2/g) (NOVA 1000e, Quantachrome Instruments, USA). Sample preheating was achieved by passing nitrogen flow for 3 h at 200 °C to remove all volatile components. The specific surface areas were determined using the BET equation with an instrumental error of 10 m^2/g. The pore volume (detection limit at standard temperature and pressure is 0.0001 cc/g) and pore size distributions (detection range of 3.5–4000 Å) were measured using the Barrett–Joyner–Halenda (BJH) cumulative pore volume method. A thermo-conductivity analyzer (TPS 2500 S, Sweden, measurement range: 0.005–1800 W/m K with relative error <5%) was used to measure the composite thermal conductivity. Fourier Transform Infrared Spectroscopy (FTIR) was performed using Frontier MIR spectrometer (PerkinElmer, SP10 STD, USA) to confirm functional groups in aerogels and composites. The flexural strength was determined by a three-point bending test on Universal Testing Machine (Shimadzu, AGS-500A, Japan) with a crosshead speed of 0.21 mm/min based on the ASTM C1341-06 method (ASTM, 1998). The cross-sectional dimensions of the specimen bar were 5 mm × 15 mm

Table 1 Characterizations of fiber-reinforced aerogel composites with respect to different fiber content

Composite	Fiber content (%)	Specific surface area (m^2/g)	Pore volume (cm^3/g)	Porosity (%)	Density (g/cm^3)	Average pore size (nm)
GF0	0	932.979	2.663	85.70	–	2.858
GF3.5	3.53	893.773	2.549	85.15	0.131	2.984
GF5	4.93	847.962	2.365	84.18	0.146	3.145
GF5&CF5	9.92	861.754	2.301	81.15	0.133	3.094
GF10	10.04	593.051	2.193	83.76	0.152	3.848
GF15	15.32	584.788	2.046	83.48	0.167	4.560
GF20	20.18	534.283	1.995	81.78	0.182	4.991
GF30	30.13	468.074	1.776	79.98	0.211	5.697
GF50	50.08	335.284	1.341	75.11	0.245	7.953

while the length of the support span was 80 mm. At least three specimens were measured for each composite and the flexural strength values were averaged from the triplicate measurements. The structure of the composites was also characterized by optical microscope (OM) (OLYMPUS, BX51, Japan). OM was equipped with built-in Koehler illumination for transmitted light 12 V, 100 W halogen bulb, a light preset switch, and light intensity LED indicator with built-in filters and a super widefield of 26.5 mm.

3 Results and discussion

3.1 Microstructure of fiber-reinforced aerogel composite

The silica aerogels originally as powders were prepared through a three-step sol-gel process, gelation, aging, and followed by APD [4, 5]. FTIR spectra confirmed the O−Si−O bonds (1,071 cm^{-1}), and Si−$(CH_3)_3$ groups (1,256 cm^{-1}, 845 cm^{-1}, and 757 cm^{-1}) which originated from TMCS with three $-CH_3$ groups. The porosity, BET surface area, and thermal conductivity of the as-prepared aerogels were 85.42%, 932.979 m^2/g, and 0.036 W/m K. These results were comparable to aerogel samples obtained from Cabot Corp (Boston, MA), by SCD, where large surface area was 750 m^2/g and low thermal conductivity was 0.033 W/m K.

Fibers as a skeleton into the aerogel were introduced to improve the aerogel's brittle structure. When the as-prepared silica alcosol was added into the mold with arranged fibers, the sol solution filled the void spaces among the fibers, enabling the formed silica gel to firmly cover the fiber from all dimensions. The ideal composite contained a robust structure while maintaining low thermal conductivity. Figure 1 a, b are optical microscope photographs of aerogel composites with GF blankets. The interwoven fiber structure was expected to be maintained in the aerogel composite, which enhanced the strength of the composite. However, intertwined fibers may still allow heat transmission through these solid GFs, resulting in relatively high heat conductivity. Figure 1c, d were optical microscope photographs of aerogel formation in the CFs after carding. To increase the gap between fibers, the sol solution was added to the well-surrounded, dispersed CFs in the mold, with each fiber apart from one another. In other words, gel molecules filled the void spaces among the CFs by aggregating on fiber surfaces while the gel network was supported by CFs. Although the CF composite with the well-dispersed stranded fibers could serve as a good heat-resistant layer, this layer was not comparably strong as interwoven layers of GF in blanket form, both functional layers could be complementary, as the strength of the composites and insulation performance was considered as a whole.

3.2 Flexural properties of the composites

Flexural strength (stress) is a measure of how much force a composite can support before breaking. Flexural modulus (Young's modulus) is a measure of rigidity, calculated by dividing the change in stress by the change in strain from the linear portion of the stress-strain curve. The results from the three-point bending tests are shown in Fig. 2. As indicated, the bending strength of the aerogel composites are associated with the amount of fibers and aerogel molecules. The stress-strain curves began with a straight-line segment that rose as strain increased, where the composites underwent only elastic deformation. These composites had nearly identical values of Young's modulus but different yield strengths. The yield strengths of the composites from the highest to the lowest were GF20 (2.97 MPa), GF10 (2.62 MPa), GF30 (1.90 MPa), GF5&CF5 (1.84 MPa), GF5 (1.55 MPa), and GF3.5 (0.92 MPa) respectively. Pure silica aerogels were not included in the bending test considering they were too fragile to sustain external force. Yet, previous study reported that yield strength of pure silica aerogel was 0.72 MPa [8]. We also noticed that GF10 exhibited much higher strength than GF5&CF5. This is most likely because the GF10 contained three layers of interwoven GF blankets while GF5&CF5 composite contained a well dispersed carding stranded CFs in the middle layer. Although composites with the carding stranded CFs tend to be weaker than composites with GF blankets, flexural strength (2.846 MPa) of GF5&CF5 composite was found higher than previous similar works [8, 14].

The composites cracked at the end of the stage and suffered from partial deformation. In fact, they could still continue to carry load at a slower rising rate after the curve was nonlinear. A rapid decline occurred after the GF-reinforced aerogel composites had reached a maximum stress. The composite with 20% GFs (GF20) exhibited the highest strength (4.39 MPa). The stress-strain curve of GF20 also showed more sharply jagged fluctuations to the failure point than other GF-reinforced aerogel composites. The composite strength also appeared to increase as fiber content increased. However, excessive fiber content led to weaker structures due to the paucity of aerogels filled in the fiber voids (GF20 (4.39 MPa) > GF30 (3.179 MPa) > GF50 (2.889 MPa)). Similar trends were also found in Wang et al [16]. and Ślosarczyk [17], where the stress-strain curves in Fig. 2 could be divided into three stages: the linear stage, the yielding stage, and the densification stage. In the first elastic stage, the load was carried by the overall material frame; in the second, inelastic stage, after the silica matrix cracks, the load is carried mainly by the fibers; and the third

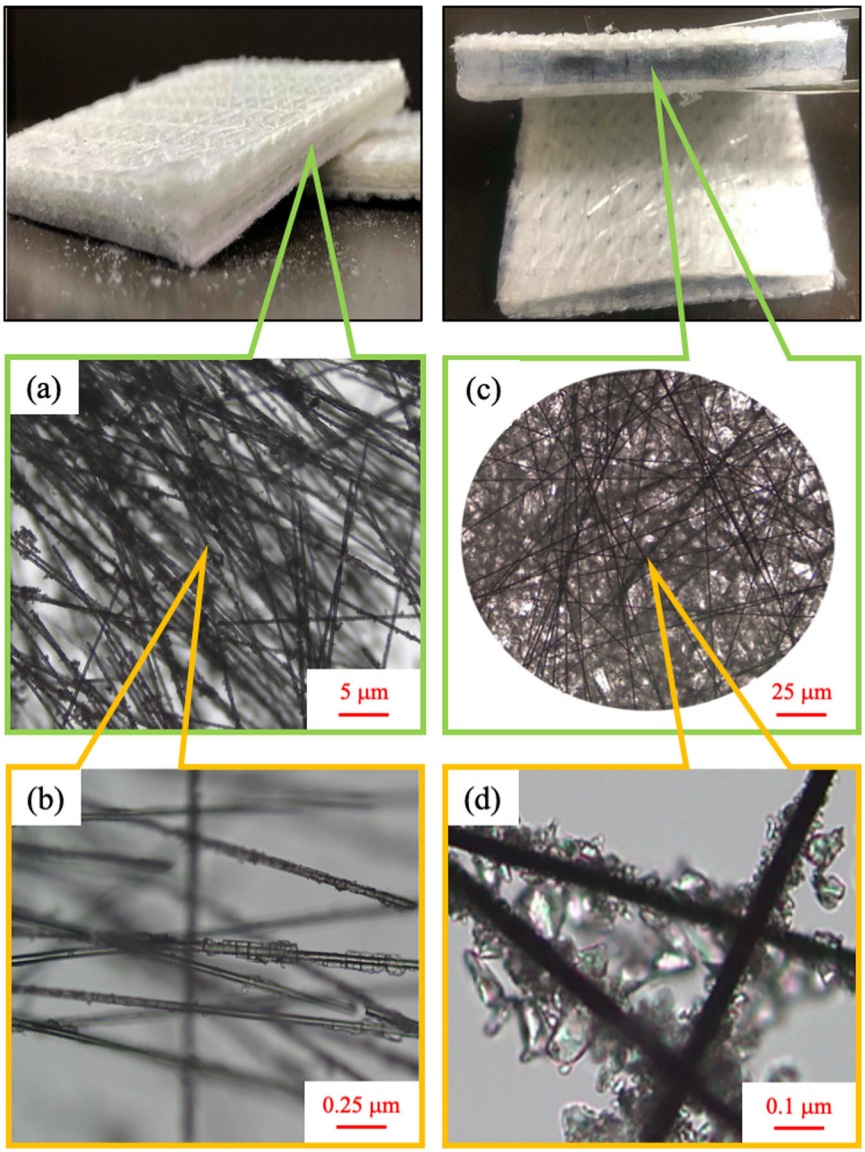

Fig. 1 Microstructure of fiber-reinforced aerogel composites: **a** GF composite at ×200 magnification; **b** GF composite at ×400 magnification; **c** CF composites at ×40 magnification; and **d** CF composites in ×200 magnification

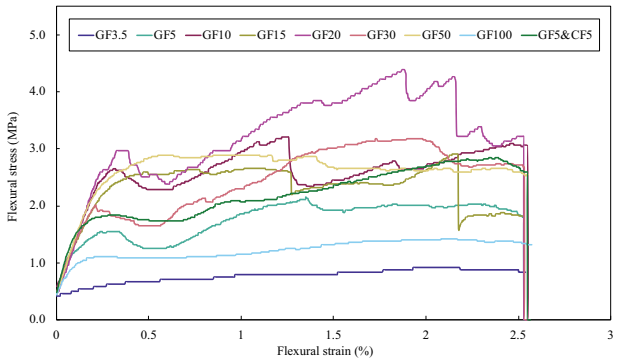

Fig. 2 Flexural stress-strain curves for composites of GF3.5, GF5, GF10, GF15, GF20, and GF30, GF50, GF100, and GF5&CF5

stage depends on the degree of composite density, fibers strength, and fibers adhesion to silica matrix. This specific conduct of composites was attributed to the formation of large clusters of aerogel nanoparticles, fiber stress relaxation, and gradual cracking and moving of the fibers from the aerogel structure.

3.3 Effects of composite fiber contents on thermal insulation performance

In general, heat transfer of aerogel compounds depends on three mechanisms: low heat conduction via the solid backbone, low heat transfer rate within the gaseous phase present in the highly porous aerogel structure, and radiative heat transfer through photons [18]. Thus, composite heat transfer is highly related to density (or solid mass to volume ratio representing the effects of conduction), porosity, and pore size (representing the effects of the free gas heat

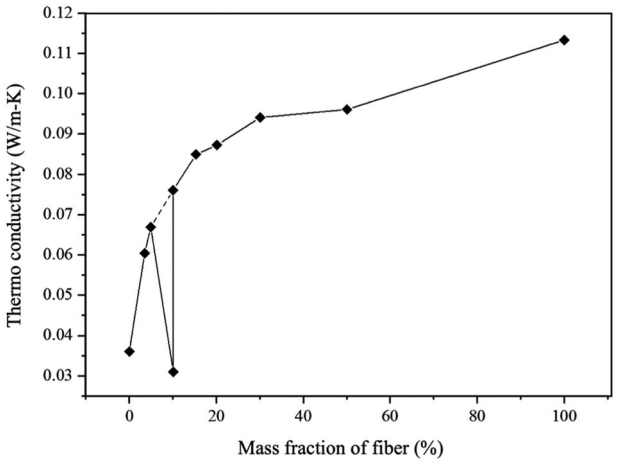

Fig. 3 Influence of fiber content on thermal conductivity of silica aerogel composites

transfer activity in the composite pores). Table 1 shows the composite density, surface area, porosity, and pore size with respect to different fiber contents. Porosity decreases as bulk density increases with the increased loadings of GFs. The composite sample with the lowest fiber content (GF 3.5) possessed the lowest bulk density (0.131 g/cm^3) and the highest porosity (85.15%). The sample with 50% GFs (GF50) showed the highest bulk density (0.245 g/cm^3) and the lowest porosity (75.11%) among all samples. Sample pore sizes varied from 1 to 16 nm while average pore diameter ranged from 2.858 to 7.953 nm, depending upon the fiber content. These results showed that aerogel composites had relatively low density and their pore sizes were smaller than the mean free path of free air molecules (70 nm for air at atmospheric pressure), both of which reflect the potential of low heat transfer rates in these aerogel samples. It was also observed that pore volume of fiber-reinforced silica aerogel composites decreased with the increasing of fiber content. This is due to the pores in the silica aerogel matrix were gradually replaced by the glass and CFs, both of which are nonporous materials. Consequently, incorporation of more glass or CFs into silica nanoparticles would result in lower porosity, pore volume, and more significant decrease of specific surface area. All these changes ultimately led to increase of average pore sizes.

Figure 3 shows the effects of composite fiber contents on thermal conductivity. The composite with the lowest GF content (GF3.5) possessed the lowest heat conductivity (0.0604 W/m K), and the composite with 50% GFs showed the highest thermal conductivity (0.0961 W/m K). For GF5, GF10, and GF20, the densities were 0.146, 0.152, and 0.182 g/cm^3, along with associated average pore sizes of 3.145 nm, 3.848 nm, and 4.991 nm, while heat conductivities were 0.0669, 0.076, and 0.0873 W/m K, respectively. As described earlier, this may be attributed to

Table 2 Composite properties with various ratios of glass fiber and carbon fiber

Fiber content (%)	Maximum stress (MPa)	Thermal conductivity (W/m·K)	Density (g/cm^3)
GF3.5 + CF5	1.988	0.0335	0.138
GF5 + CF5	2.846	0.031	0.133
GF10 + CF5	2.909	0.0513	0.149
GF5 + CF3.5	2.174	0.042	0.144
GF5 + CF10	2.909	0.0322	0.135
GF5 + CF15	2.342	0.032	0.135

the fact that the fiber contacts among fiber blankets provide other paths of conducting heat to increase heat conductivity. In most cases, thermal conductivity increased as GF content increased. However, thermal conductivities were still below typical thermal insulators (0.1 W/m K). To further inhibit heat transmission through the composites, a heat insulation layer was inserted between two GF blanket layers; when carding CFs was introduced to the middle layer between two GF layers, surprisingly, the composite of 10% fiber (5% GF and 5% CF) exhibited more thermally insulative properties than GF composites. Its value, 0.031 W/m K, was similar to that of the pure aerogel, 0.036 W/m K. The results indicated that the reinforcements in the aerogel matrix could be purpose driven. When the composites are designed for structural purposes, stronger fiber content can be amended, such as fiber blankets. Likewise, an insulation layer, such as well-distributed carding fibers, may be included for heat insulation purposes.

It seems applicable that aerogel composites can be assembled using a carding CF as the heat insulation layer and GF layers for strengthening purposes, with 10–20% of fibers optimally. Table 2 demonstrates that when carding CF 5% was introduced and sandwiched between two GF layers, the strength of the composite increased with the increase of GF content with heat conductivity ranging from 0.031 to 0.0513 W/m K. As CF content varied from 3.5 to 15% when GF was 5%, both flexural strength and heat conductivity increased with the increase of CF content. More specifically, the heat conductivity changed from 0.032 to 0.042 W/m K, indicating that CFs play a significant role on composite strength and heat transfer rate. In this case, CFs may be less cost-effective and absorb more heat due to radiation.

Furthermore, composites including GF3, GF5, GF5&CF5, and G10 were chosen to evaluate their thermal performance in a small-sized hot-box with a solar simulator lamp, detailed experimental information could be found in Alvarez et al [19]. and Lee et al [20]. Under the radiation of a halogen lamp of electric power of 500 W/110 V, samples

were placed on the sample frame, and temperatures were recorded until a steady state was achieved. The surface temperature on both sides of the samples reached a steady state at about 7200 s. The temperature on the top surface of samples was greater than that on the other side, due to the heat-absorptive ability of the sample materials. The steady temperature on exterior surface of the samples was 81.18 °C, 76.69 °C, 99.62 °C, and 79.81 °C, and on the bottom side was 34.76 °C, 38.14 °C, 37.12 °C, and 38.31 °C respectively. Noticeably, the temperature difference of GF5&CF5 composite between top and bottom surfaces was the highest (56.74 °C) among selected composites, implying that the middle CF layer may play a critical role in low heat conductivity. However, high temperature difference may lead to heat accumulation on the top surface of GF layer, which should be taken into consideration for their future application. In brief, the heat insulation and strength were significantly improved by adding CF. The composite content with GF 5% and CF 5% was shown to be the most optimal loading in terms of thermal conductivity and strength. This recipe can be useful when designing versatile composites, considering different heat conductivities and bending strengths applied in different industrial applications. However, attention should be also drawn to the composites for uses at high temperature; adopting higher heat-resistant fibers may be considered an option [21]; more testing is also necessary as their mechanical strength, specific surface area, and heat conductivity would vary under such environment.

4 Conclusion

This work investigated the heat insulation performance of silica aerogels composited with different ratios of GF and CF. Aerogels are well known for their relatively low heat conductivities despite their low strength for a wide range of industrial applications. Meanwhile, glass and CFs have been widely used to reinforce their structure. The aerogels and composites were prepared via a sol-gel method with APD. The results show that, though thermal conductivity increased with the increasing GF content, the flexural strength increased with increased GF loading, and reached its highest value when GF content was 20%. To promote both heat insulation performance and strengthening the composite structure, 5% CF inserted between the two 5% GF layers appeared to be the most optimized condition. The flexural strength of GF5&CF5 was 2.846 MPa, exhibiting better strength than previous studies. Besides, thermal conductivity was remarkably low (0.031 W/m K), similar to that of the pure aerogel (0.036 W/m K). Composites reinforced with various ratios of combined glass/CFs were also characterized, which demonstrated better flexural strength and lower thermal conductivity than composites with only GFs. Based on our findings, 10% fiber composite with a sandwiched alignment was recommended, in which 5% carding CF was used as the heat insulation layer and two GF blanket layers as the structure strengthening layers. As examined in a simulated solar radiation system, GF5&CF5 exhibited the highest heat insulation capability among selected samples. This work provides an alternative method to prepare versatile fiber-reinforced aerogel composites that could be useful in future industrial application.

Acknowledgements The authors wish to thank the ministry of science and technology in Taiwan for their financial support under project MOST 109-2221-E-214-002 and ISU project ISU 108-02-02A, without which this work would have been very difficult.

Compliance with ethical standards

Conflict of interest The authors declare that they have no known competing financial interests or personal relationships that could have appeared to influence the work reported in this paper.

Publisher's note Springer Nature remains neutral with regard to jurisdictional claims in published maps and institutional affiliations.

References

1. Cotana F, Pisello AL, Moretti E, Buratti C (2014) "Multipurpose characterization of glazing systems with silica aerogel: In-field experimental analysis of thermal-energy, lighting and acoustic performance.". Build Environ 81:92–102
2. Gao T, Jelle BP, Ihara T, Gustavsen A (2014) "Insulating glazing units with silica aerogel granules: the impact of particle size.". Appl Energy 128:27–34
3. Kistler SS (1931) "Coherent expanded aerogels and jellies". Nature 127(3211):741–741
4. Rao AP, Rao AV, Pajonk GM (2007) "Hydrophobic and physical properties of the ambient pressure dried silica aerogels with sodium silicate precursor using various surface modification agents". Appl Surf Sci 253(14):6032–6040
5. Shewale PM, Rao AV, Gurav JL, Rao AP (2009) "Synthesis and characterization of low density and hydrophobic silica aerogels dried at ambient pressure using sodium silicate precursor". J Porous Mater 16(1):101–108
6. Deng Z, Wang J, Wu A, Shen J, Zhou B (1998) "High strength SiO2 aerogel insulation". J Non-crystalline Solids 225:101–104
7. Wei TY, Lu SY, Chang YC (2009) "A new class of opacified monolithic aerogels of ultralow high-temperature thermal conductivities". J Phys Chem C 113(17):7424–7428
8. Wu H, Liao Y, Ding Y, Wang H, Peng C, Yin S (2014) "Engineering thermal and mechanical properties of multilayer aligned fiber-reinforced aerogel composites". Heat Transf Eng 35(11-12):1061–1070
9. "Aspen Aerogels Industrial Aerogels insulation". *Aspen Aerogels*, http://www.aerogel.com. Accessed 11 July 2019
10. "Cabot Corporation". *CABOT*, http://www.cabotcorp.com. Accessed 15 Feb 2017
11. Yang X, Sun Y, Shi D, Liu J (2011) "Experimental investigation on mechanical properties of a fiber-reinforced silica aerogel composite". Mater Sci Eng: A 528(13-14):4830–4836

12. Yang X, Sun Y, Shi D (2012) "Experimental investigation and modeling of the creep behavior of ceramic fiber-reinforced SiO2 aerogel". J Non-crystalline Solids 358(3):519–524
13. Zhou T, Cheng X, Pan Y, Li C, Gong L, Zhang H (2018) Mechanical performance and thermal stability of glass fiber reinforced silica aerogel composites based on co-precursor method by freeze drying. Appl Surf Sci 437:321–328
14. Shafi S, Tian J, Navik R, Gai Y, Ding X, Zhao Y (2019) "Fume silica improves the insulating and mechanical performance of silica aerogel/glass fiber composite". J Supercrit Fluids 148:9–15
15. Standard, ASTM 2004. Annual book of ASTM standards. American Society for Testing and Materials Annual, Philadelphia, PA, USA, 4 (04.08)
16. Wang, X 2006. "Base research on the application of nanoporous SiO2 aerogel based thermal insulation composites." National University of Defense Technology, *Changsha*
17. Ślosarczyk A (2017) "Recent advances in research on the synthetic fiber based silica aerogel nanocomposites". Nanomaterials 7 (2):44
18. Ebert, HP (2011). Thermal properties of aerogels. In Aerogels handbook. Springer, New York, NY, p 537–564
19. Alvarez G, Palacios MJ, Flores JJ (2000) "A test method to evaluate the thermal performance of window glazings". Appl Therm Eng 20(9):803–812
20. Lee SK, Chen HJ, Fan KS, His HC, Horng RS (2014) "Thermal performance and durability properties of the window glazing with exterior film(s)". Indoor Built Environ 23 (8):1163–1176
21. Berger, M and Bunsell, A (eds) (1999) Fine Ceramic Fibers. CRC Press. p 239–258. https://books.google.com/books/about/Fine_Ceramic_Fibers.html?id=xH93Gn5pIxQC